

⁴A. G. Redfield, Phys. Rev. **98**, 1787 (1955).

⁵D. Barnaal and I. J. Lowe, Abstracts from 4th OCEANS, Mellon Institute, Pittsburgh, Pennsylvania, 1963 (unpublished); following Letter [Phys. Rev. Letters **11**, 258 (1963)].

⁶The calculation of $M_z(\infty)/M_z(0)$ requires a knowledge

of the orientation-dependent quantity, H_l , the local field in the crystal. For details see C. P. Slichter and W. C. Holton, Phys. Rev. **122**, 1701 (1961); Walter I. Goldberg, Phys. Rev. **128**, 1554 (1962).

⁷S. Clough, K. W. Gray, and I. R. McDonald (to be published).

EFFECTS OF ROTATING MAGNETIC FIELDS ON FREE-INDUCTION DECAY SHAPES*

D. Barnaal and I. J. Lowe

Department of Physics, University of Pittsburgh, Pittsburgh, Pennsylvania

(Received 5 August 1963)

The lengthening of a nuclear magnetic resonance free-induction decay by applying a rotating magnetic field to a spin system has been observed.

In order to find out how such an effect might occur, let us analyze the behavior of a set of N particles with spin s and magnetogyric ratio γ , placed in a magnetic field $H_1(\cos\omega t\hat{i} + \sin\omega t\hat{j}) + H_0\hat{k}$. The spin system, when referred to a frame of reference rotating about the z axis with angular speed ω , has the following magnetic Hamiltonian¹:

$$\mathcal{H}_1 = -\gamma\hbar \sum_{j=1}^N [H_1 s_{jy} + (H_0 + \omega/\gamma)s_{jz} + \frac{1}{2} \sum_{j \neq k} (A_{jk} \hat{s}_j \cdot \hat{s}_k + B_{jk} s_{jz} s_{kz})]. \quad (1)$$

Only the time-independent terms of the interaction between the spins, as viewed from the rotating reference frame, are listed, since for large H_0 these are the only magnetic terms that determine the free-induction decay shape.¹

In this rotating coordinate system (rotating coordinate system No. 1), there is a magnetic field

$$\vec{H}_{\text{eff}} = H_1 \hat{y} + (H_0 + \omega/\gamma) \hat{z} \quad (2)$$

that makes an angle $\theta = \arctan H_1/(H_0 + \omega/\gamma)$ with the z axis. By making a transformation to a coordinate system rotating about \vec{H}_{eff} with angular speed $\omega_{\text{eff}} = -\gamma H_{\text{eff}}$ (rotating coordinate system No. 2), one obtains a new magnetic Hamiltonian whose time-independent terms are

$$\mathcal{H}_2 = \frac{1}{2} (3 \cos^2 \theta - 1) \left[\frac{1}{2} \sum_{j \neq k} B_{jk} (s_{jz} s_{kz} - \frac{1}{3} \hat{s}_j \cdot \hat{s}_k) \right] + \frac{1}{2} \sum_{j \neq k} (A_{jk} + \frac{1}{3} B_{jk}) \hat{s}_j \cdot \hat{s}_k. \quad (3)$$

If there are only magnetic dipole interactions between the spins, $A_{jk} = -\frac{1}{3} B_{jk}$, making the second

summation of (3) vanish. The omission of the time-dependent terms in \mathcal{H}_2 is a reasonable approximation only if $|\omega_{\text{eff}}|$ is much greater than the regular nmr absorption linewidth.

For the case of $H_1 = 0$, the rate of decay of the component of magnetization perpendicular to $H_0 \hat{z}$ is determined by \mathcal{H}_1 and is just the normal free-induction decay in rotating reference frame No. 1.² Using the same arguments as in reference 2, we conclude that as long as spin-lattice relaxation effects may be ignored, the rate of decay of any component of magnetization perpendicular to \vec{H}_{eff} is determined by \mathcal{H}_2 for $|\omega_{\text{eff}}|$ large enough. For pure dipolar interactions between the spins, \mathcal{H}_2 has the same form as \mathcal{H}_1 except for a multiplying factor of $\frac{1}{2}(3 \cos^2 \theta - 1)$. Thus a free-induction decay (f.i.d.) about \vec{H}_{eff} should have the shape of a normal f.i.d. about $H_0 \hat{z}$, with the time axis stretched by a factor of $2/|3 \cos^2 \theta - 1|$. For $\theta = 90^\circ$, one need only replace t in the free-induction decay formula² by $\frac{1}{2}\tau$, while for $\theta = \arccos 1/\sqrt{3} \approx 54.7^\circ$, the magnetization perpendicular to \vec{H}_{eff} will not decay at all (within the limits that one can ignore the time-dependent terms not listed in \mathcal{H}_2).

We have been able to include the time-dependent terms, omitted in the above discussion of \mathcal{H}_2 , in the computation of the rate of decay of magnetization perpendicular to \vec{H}_{eff} for the special case that $s = \frac{1}{2}$, that $\theta = 90^\circ$, and that each spin interacts with only one other spin (such as approximately occurs in gypsum). We find that $M_x(t)$, the x component of magnetization in the first rotating coordinate system, is given by the formula

$$M_x(t) = M(0)(\omega_1/\Omega) \sin \tau \Omega \cos(B_{12}/2\hbar)(t + \frac{1}{2}\tau), \quad (4)$$

where $\Omega = [(B_{12}/4\hbar)^2 + \omega_1^2]^{1/2}$, $\omega_1 = \gamma H_1$, $M(0)$ is the equilibrium magnetization just before the rotating magnetic field H_1 is turned on, τ is the length of time H_1 is on, and t is the length of time between

the turnoff of H_1 and the measurement of M_x . For $\hbar\omega_1 \gg B_{12}$, Eq. (4) reduces to

$$M_x(t) = M(0) \sin\omega_1\tau \cos[(B_{12}/2\hbar)(\frac{1}{2}\tau + t)], \quad (5)$$

which is what one would have concluded from the previous arguments based upon the secular terms of \mathcal{H}_2 . Equation (4) shows that the nonsecular terms do make a contribution to the time rate of change of magnetization while H_1 is on if H_1 is not large enough. It also shows that the shape of the f.i.d. following the turnoff of H_1 is independent of ω_1 (although its initial amplitude does depend upon ω_1). The only parameter in the free-induction decay shape that depends upon H_1 is the f.i.d. origin, occurring at $\frac{1}{2}\tau$. We have not yet proven this result for the n -spin case, but we do find it to be true experimentally for the n -spin case to within the accuracy of our measurements.

An experiment to determine the effect of pulse length on the subsequent f.i.d. has been carried out in gypsum, calcium fluoride, and ice for the case of $\theta = \frac{1}{2}\pi$. A single rf pulse at the Larmor frequency of the spin system (10 Mc/sec) was applied to a sample in equilibrium, and the resulting f.i.d. shape after the end of the pulse was recorded. The rf pulse length was varied from about 1 to 18 μsec , and H_1 ranged from 3 to 30 gauss for these pulse lengths. These field strengths compare to a root second moment of 3.5 gauss for the [100] direction of calcium fluoride, and a nominal 5 gauss for the gypsum and

ice crystals.

In all three samples, the f.i.d. envelope oscillates about zero several times before dying out. The position of the points where the f.i.d. envelope crosses the axis is one of the most accurately measurable characteristics of the f.i.d. shape, and these were measured with respect to their occurrence after the end of the rf pulse. The end of the rf pulse was defined to be the nominal half-power point of the rf pulse, and the pulse length was measured with respect to the half-power points. The rise and fall times of the rf pulses were approximately $\frac{1}{2} \mu\text{sec}$.

Figure 1 shows the occurrence of the f.i.d. zero points versus rf pulse length for a single crystal of gypsum. Three sets of the data are shown, corresponding to three different orientations of the crystal with respect to the static magnetic field. For two of these orientations, a second zero is also plotted on the graph. All the lines on the graph were drawn to have slope $\frac{1}{2}$. Thus if the rf pulse length is increased by 2 μsec ; the f.i.d. zeros occur 1 μsec earlier with respect to the end of the pulse.

Figure 2 shows the results of the experiment on a single crystal of calcium fluoride. The time of occurrence of first f.i.d. zero relative to the end of the rf pulse is plotted vs rf pulse length for the case of the static magnetic field along the [100] direction, which is the direction of the largest root second moment. Again the line drawn has slope $\frac{1}{2}$.

Gypsum and calcium fluoride were chosen as samples because gypsum has a characteristic two-

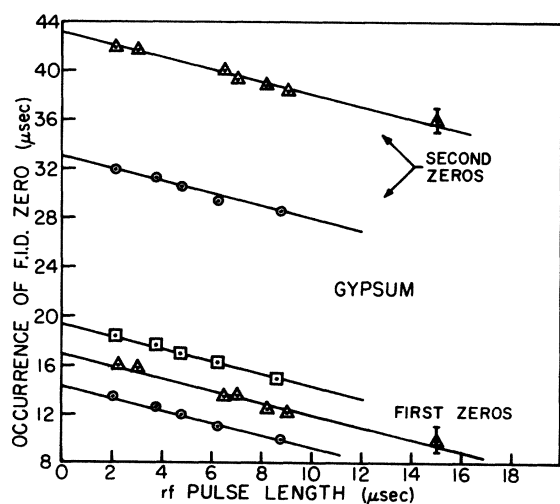


FIG. 1. Plot of time of occurrence of f.i.d. zero (measured from end of rf pulse) versus rf pulse length, for a single crystal of gypsum. Data for three orientations of the crystal relative to $H_0\hat{z}$ are shown.

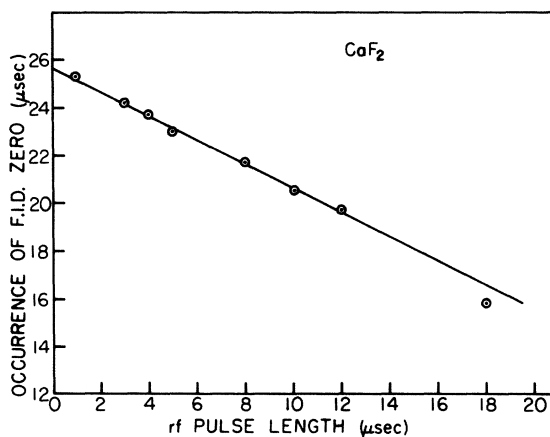


FIG. 2. Plot of time of occurrence of first f.i.d. zero (measured from end of rf pulse) versus rf pulse length, for a single crystal of calcium fluoride. $H_0\hat{z}$ is along the [100] crystalline axis.

spin interaction line shape, while calcium fluoride provides the contrasting situation of a simple cubic lattice where all spins are equivalent. In both materials, when the H_1 field was varied from 3 to 30 gauss for a given pulse length, no shift could be observed in the f.i.d. zeros. The entire visible calcium fluoride f.i.d. shape was also checked for distortion for many pulse-length and field-strength combinations. None was found within the 7% reading accuracy of our data.

The shift of the crossing point vs pulse length was also checked for the proton line shape of a single crystal of ice, and polycrystalline ice. Again a line of slope $\frac{1}{2}$ fitted the data very well. The polycrystalline sample was also examined at -5°C where the internal motion washes out the zeros and substantially changes the f.i.d. shape to that of a Gaussian. Again the line shape was found to be undistorted for pulse lengths of from 2 to 10 μsec , provided the f.i.d. shape was assumed to begin decaying at the center of the rf pulse. The $1/e$ point of the Gaussian was 16 μsec .

From the gypsum and ice data it appears that the two-spin calculation is quantitatively verified, and the calcium fluoride data seems to indicate that to a high degree of accuracy the same result applies to the n -spin case. We thus conclude that

while the H_1 field is on, the rate of decrease of magnetization is reduced by a factor of two. These experiments also show that for long rf pulses, the undistorted f.i.d. is observed provided the time origin is taken to be the center of the rf pulse.

A final note: It is easily proven that for the spin system described by \mathcal{K}_1 , and for $\theta = 90^\circ$,

$$M_x(\tau) = -(1/\omega_1)(\partial/\partial\tau)M_z(\tau).$$

From our measurements $M_x(t)$, we obtained information about $M_x(\tau)$. Thus our measurements are closely related to those of Goldburg and Lee as presented in the previous paper.³ Since we measured line shapes and not line amplitudes, our measurement technique is not sensitive to the effects of time-dependent terms in \mathcal{K}_2 .

*This work was supported by grants from the Alfred P. Sloan Foundation, the National Science Foundation, and the U. S. Air Force Office of Scientific Research.

¹A. Abragam, The Principles of Nuclear Magnetism (Clarendon Press, Oxford, England, 1961).

²I. J. Lowe and R. E. Norberg, *Phys. Rev.* **107**, 46 (1957).

³W. I. Goldberg and M. Lee, preceding Letter [*Phys. Rev. Letters* **11**, 255 (1963)].

MAGNETOMORPHIC OSCILLATIONS IN THE HALL EFFECT AND MAGNETORESISTANCE IN CADMIUM*

N. H. Zebouni, R. E. Hamburg, and H. J. Mackey

Louisiana State University, Baton Rouge, Louisiana

(Received 12 August 1963)

Large-amplitude oscillations periodic in the magnetic field have been found in the Hall resistivity ρ_{21} of cadmium single crystals at liquid helium temperatures¹ (see Figs. 1 and 2). Oscillations of the same period and comparable amplitude have been observed also in the transverse magnetoresistivity ρ_{11} . The oscillations differ in phase by about 55° or 130° . These phenomena appear to be the size-effect oscillations predicted by Sondheimer² and first observed by Babiskin and Siebenmann.³

Samples and experimental conditions.—Two single crystals, Cd1 and Cd2, were cut in the form of rectangular plates from a zone-refined cadmium bar (Tadanac).⁴ The crystals are oriented with the hexagonal axis perpendicular to the large faces and the binary axis at about 17° with respect to the longest dimensions. The di-

mensions of the samples are, for Cd1, $0.8 \times 5 \times 19$ mm; for Cd2, $2.3 \times 5.5 \times 15$ mm.

The experimental arrangements were such that the magnetic field was parallel to the hexagonal axis (normal to the large faces of the plate) and the current was in the direction of the longest dimension. Changes in voltage could be measured with a precision of $\pm 10^{-9}$ V.

Size dependence.—The period P and the amplitude of the oscillations $|\tilde{\rho}_{21}|$ in ρ_{21} decrease as thickness increases, as seen in Table I and Fig. 3(b). The onset of oscillations occurs at a lower field in the thick sample, Cd2, than in Cd1.

Orientation dependence.—The magnetic field was rotated in the plane normal to the length of the sample. As the angle ϕ between the hexagonal axis and the magnetic field direction is in-